

DETERMINATION OF OPTICAL CONSTANTS AND MECHANICAL PROPERTIES OF THIOUREA BASED METAL COMPLEX CRYSTAL

P. Chellapappa¹, Sutapa Guosh^{1*}

^{1*}Department of Physics, PRIST University, Chennai Campus, Manamai, ECR, Mahabalipuram 603102. Tamilnadu, India

Abstract - Bis-thiourea stannous chloride dihydrate (BTSCD) crystal were grown by solution growth method in the molar ratio 2:1 at room temperature. Transparent and defect free crystal of BTSCD were harvested in the period of 35-45 days with dimension 5mm × 4mm × 2mm. Single crystal XRD analysis revealed that the BTSCD crystal belongs to Orthorhombic crystal system. The sharp and well defined Bragg peaks observed in the powder XRD pattern confirm the crystalline nature of BTSCD crystal. The presences of functional groups in the grown BTSCD crystal were identified by FT-IR analysis. . UV-visible analysis was carried out to determine the lower cut off wavelength. Also optical constants like Band gap (E_g), Refractive index (n), Reflectance (R), Extinction coefficient (K) and Electric susceptibility were determined from UV-VIS-NIR spectrum Second harmonic generation (SHG) of powdered BTSCD sample was tested using Nd: YAG laser and is found to be 0.55 times that of potassium dihydrogen orthophosphate. The mechanical strength of the BTSCD crystal was evaluated and it describes that the Vickers hardness number of BTSCD is found to be increase with the applied load. The work hardening co-efficient (n) has been calculated from the slope of straight line between log P and log d. The dielectric study of BTSCD was carried out as a function of frequency at different temperature.

Key Words: Solution growth method, XRD, Fluorescence spectral study, SHG, Hardness.

1. INTRODUCTION

The search for new non-linear optical materials for tailor made device application had been increasing from the last few decades because of their potential industrial applications especially in the field of photonics for optical switching, optical modulators, data storage devices, telecommunication and high density optical data storage [1,2]. The importance of amino acids and their salts belongs to a family of organic materials that have wider NLO applications [3-5]. Amino acids contain a deprotonated carboxylic acid group (COO⁻) and protonated amino group (NH₃⁺). This dipolar nature exhibits peculiar physical and chemical properties in amino acids, thus make them ideal candidate for NLO applications [6].

Thiourea molecule is an interesting inorganic matrix modifier due to its large dipole moment and its ability to form an extensive network of hydrogen bonds [7]. The nonlinear optical properties of some of the complexes of

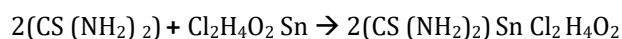
thiourea, such as bis-thiourea cadmium chloride (BTCC), bis-thiourea zinc chloride (BTZC), and potassium thiourea bromide (PTB) have gained significant attention in the last few years [8,9] because both organic and inorganic components in it contribute to the process of second harmonic generation. The centrosymmetric thiourea molecule, when combined with inorganic salt yield non-centrosymmetric complexes which has the nonlinear optical properties [10-12].

In the organic class α-amino acids exhibit some specific features such as molecular chirality, weak vanderwaals, hydrogen bonds and the absence of strongly conjugated bonds, wide transparency ranges in visible and UV spectral region and zwitterionic nature of the molecule which favours crystal hardness [13-16]. The present research article focused on synthesis, growth and characterization of Bis-thiourea stannous chloride dihydrate crystal by solution growth method.

2. EXPERIMENTAL PROCEDURE

2.1. Synthesis of BTSCD

BTSCD single crystals were synthesized using Bis-thiourea (AR Grade, Merck) and stannous chloride (AR grade, Merck) in deionized water by stoichiometric ratio 2:1 according to the following chemical reaction,



2.2. Crystal Growth of BTSCD

The prepared BTSCD solutions were stirred vigorously for 6 hours using magnetic stirrer. High degree of purity of synthesized salts was achieved by successive recrystallization process and filtration. The saturated solution of BTSCD was filtered using whatmann filter paper to remove impurities. This super saturated solution of BTSCD was tightly covered with polyethylene sheet, to keep out dust before it was allowed to evaporate at room temperature. After 15 to 20 days good quality seed crystal of BTSCD were obtained. The good quality and defect free seed crystal of BTSCD was selected for bulk growth. The BTSCD crystal of average dimension 5×4×2 mm³ has been harvested in the period of 35 to 45 days and the grown crystals are highly transparent. As grown crystal of BTSCD was shown in Figure 1.



Figure 1. As grown crystal of BTSCD

2. CHARACTERIZATION

2.1. Single crystal X-ray diffraction analysis of BTSCD crystal

BTSCD crystal was subjected to single crystal X-ray diffraction analysis using ENRAF NONIUS CAD 4-F single X-ray diffractometer with $MOK_{\alpha}(\lambda=0.717\text{\AA})$ radiation. The calculated lattice parameter values are $a = 5.15\text{\AA}$, $b = 7.76\text{\AA}$ and $c = 13.67\text{\AA}$, $\alpha = \gamma = 90^{\circ}$ and Volume $V = 546.30\text{\AA}^3$, which reveals that the grown BTSCD crystal crystallizes in orthorhombic crystal system.

2.2. Powder X-ray diffraction analysis of BTSCD crystal

A powder sample of Bis-thiourea stannous chloride dihydrate (BTSCD) was analyzed using BRUCKER Germany (Model D8 advance) X-ray diffractometer $CuK\alpha$ ($\lambda=1.5405\text{\AA}$) radiation. The powder XRD pattern is shown in Figure 2. From the powder XRD pattern, a well defined Bragg's peak confirms the crystalline nature of the grown BTSCD crystal.

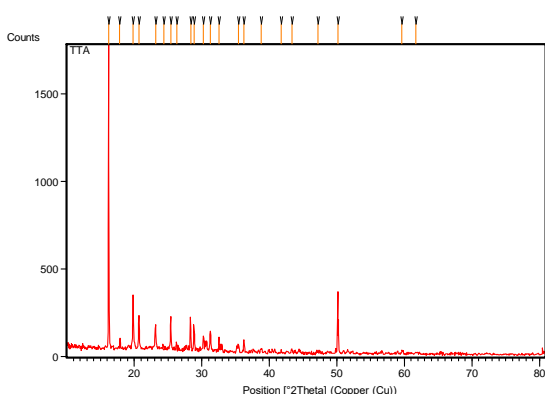


Figure 2. Powder XRD pattern of BTSCD crystal

2.3. FTIR spectral analysis

A freshly crushed powder of BTSCD crystal was subjected to FTIR studies using thermo Nicolect v-200 FTIR spectrometer by KBr pellet method in the range $500-4000\text{ cm}^{-1}$. The presences of functional groups are identified by FTIR

spectrum which is shown in Figure 3. The absorbed frequencies and their assignment of BTSCD crystals are shown in the Table 1.

The broad band in the higher energy region around 3381 cm^{-1} is due to NH_2 asymmetric stretching. The strong but broad peaks observed at 3108 cm^{-1} due to presence of C-H symmetric stretching. The C-N stretching and bending identified at 2016 cm^{-1} and respectively. The absorption band at $1575, 1525$ and 914 cm^{-1} is due to the N-C-N stretching. The peak at 1144 cm^{-1} is attributed to C=H bending. The C-C-N symmetric stretching is found at 791 cm^{-1} . The band appearing at 736 cm^{-1} infers the C-O-H stretching. The COO^- symmetric stretching was observed at 653 cm^{-1} . The absorption peak at 555 cm^{-1} is due to the C-Cl stretching. The S-C-N symmetric stretching was found at 478 cm^{-1} . The assignments confirm the presence of various functional groups present in the material.

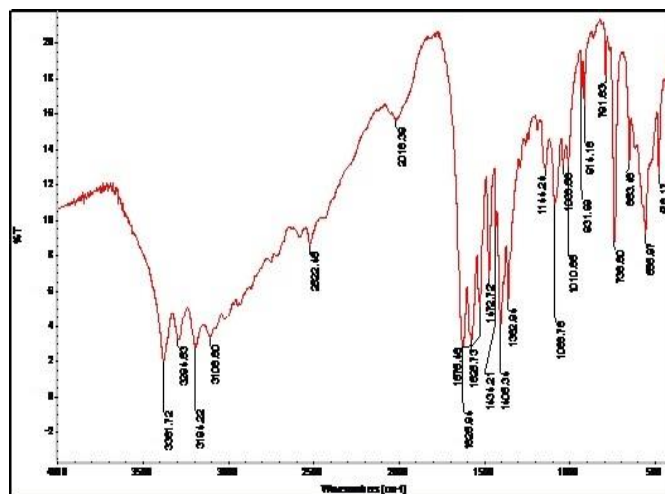


Figure 3. FTIR spectrum of BTSCD crystal

Table 1. Wavenumber assignments of BTSCD crystal

Wavenumber cm^{-1}	Assignments
3381	NH_2 asymmetric stretching
3294,3108	NH_2 symmetric stretching
2522	C-H stretching
2016	C-N stretching
1575	NCN stretching
1625	NH_2 bending
1525,1472	N-C-N stretching vibration
1434	C=S asymmetric stretching
1406,1038	C=S stretching

1362	C=H bending
1144	CH ₃ symmetric stretching
1010	C-C stretching
931	C-H symmetric stretching
791	C-C-N symmetric stretching
736	C-O-H stretching
653	COO ⁻ symmetric stretching
555	C-Cl stretching
478	S-C-N symmetric bending

3.4. Linear optical study

The optical transmission spectrum of BTSCD crystal was recorded in the range 200-1000 nm using Perkin Elmer Lambda 35 UV/VIS spectrometer. Figure 4, shows the optical transmittance spectrum of BTSCD crystal. From the spectrum, it is evident that the grown crystal has a very low cutoff wavelength of 214 nm. There is no absorption in the visible region. This lower cutoff is well suited for SHG and other application in green region.

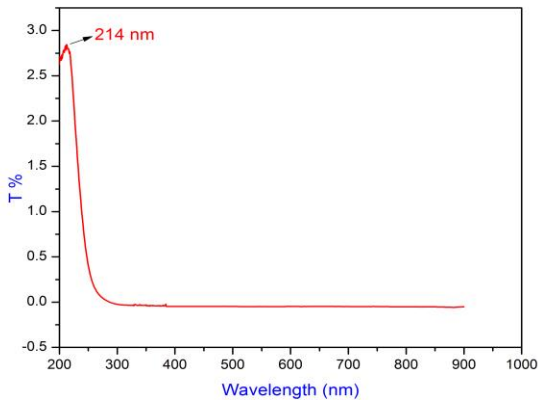


Figure 4. Opticl transmission Spectrum of BTSCD crystal

3.5. Determination of optical band gap (Eg)

The dependence of optical absorption coefficient on photon energy helps one to study the band structure and the type of transition of electrons [17]. The optical absorption coefficient (α) was calculated from transmittance using the following relation.

$$\alpha = \frac{1}{d} \log \left(\frac{1}{T} \right)$$

Where T is the transmittance and d is the thickness of the crystal. As a direct band gap material, the crystal under study

has an absorption coefficient (α) obeying the following relation for high photon energies (hv).

$$\alpha = \frac{A(h\nu - E_g)^{\frac{1}{2}}}{h\nu}$$

Where E_g is the optical band gap of the crystal and A a constant. The plot of variation of $(\alpha \cdot h\nu)^2$ versus $h\nu$ is shown in figure 5. Optical band gap was evaluated by extrapolation of the linear part [18]. The band gap (E_g) is found to be 5.1 eV. As a consequence of wide band gap, the grown crystal has large transmittance in the visible region [19].

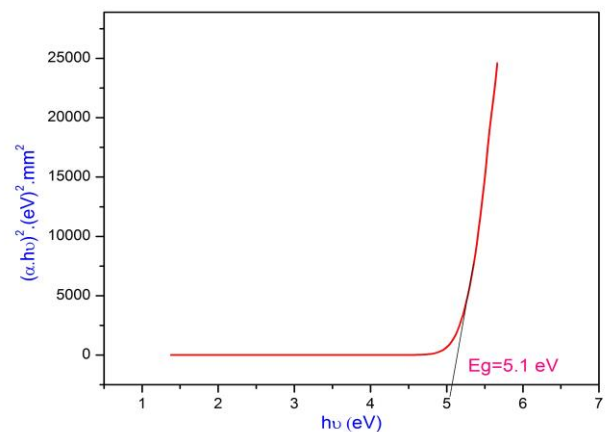


Figure 5. Tauc's plot of BTSCD crystal

Extinction coefficient (K) can be obtained from the following equation

$$K = \frac{\lambda \alpha}{4\pi}$$

The extinction coefficient as a function of absorption coefficient (α) is shown in Figure 6. The transmittance (T) is given by [20]

$$T = \frac{(1-R)^2 \exp(-\alpha t)}{1-R^2 \exp(-2\alpha t)}$$

The reflectance (R) in terms of the absorption coefficient can be obtained from the above equation. Hence,

$$R = \frac{\exp(-\alpha t) \pm \sqrt{\exp(-\alpha t) T - \exp(-3\alpha t) + \exp(-2\alpha t) T^2}}{\exp(-\alpha t) + \exp(-2\alpha t) T}$$

The refractive index (n) can be determined from reflectance data using the equation.

$$n = \frac{-(R + 1) \pm 2\sqrt{R}}{(R - 1)}$$

The absorption coefficient versus reflectance is shown in the Figure 7. Figure 8 represents the variation of refractive index as a function of wavelength. The refractive index (n) decreases with increase in wavelength indicates that the grown sample absorbs at lower wavelength region. The variation of n and K values with respect to wavelength reveals the interaction of photon with electron. The refractive index 'n' is 1.642 at 1000 nm and the refractive index is strongly dependent on wavelength.

The electrical susceptibility (χ_c) can be calculated using the following relation,

$$\chi_c = \epsilon_r - 1$$

$$(or) \quad \chi_c = n^2 - 1 \quad (i.e., \epsilon_r = n^2)$$

Hence, Susceptibility = 1.69.

Since electrical susceptibility is greater than 1, the material can be easily polarised when the incident light is more intense.

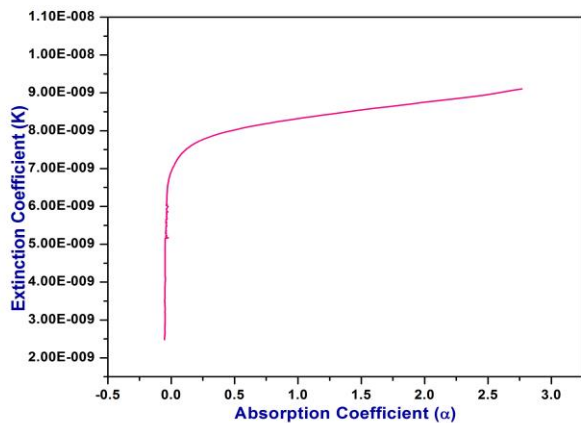


Figure 6. A plot of extinction coefficient versus absorption coefficient

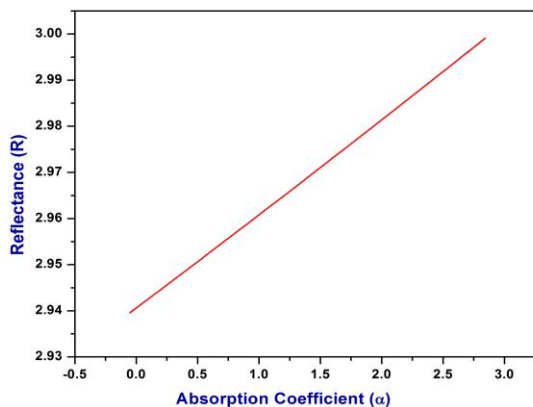


Figure 7. Absorption coefficient Vs reflectance for BTSCD crystal

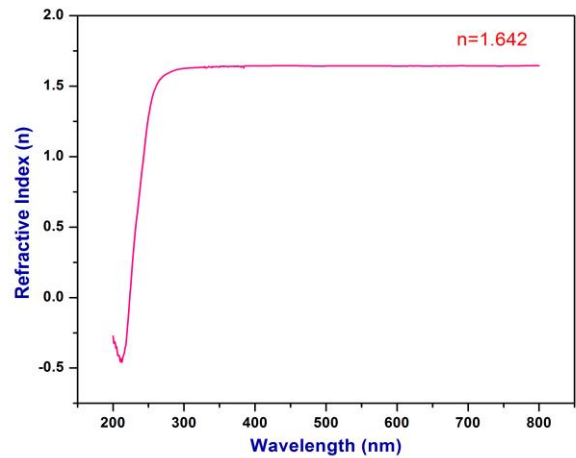


Figure 8. Plot of refractive index versus photon energy for BTSCD crystal

3.6. Nonlinear Optical Study

The powder sample of BTSCD was subjected to KURTZ and PERRY techniques. A Q-switched Nd: YAG laser emitting 1.06 μm with power density up to 1 GW/cm^2 was used as a source to illuminate the powdered sample. The sample of good graded crystalline powder with average particle size of about 90 μm sandwiched between two glass slides using copper spacers of 0.4mm thickness. A laser was produced as a continuous laser pulses with repetition rate of 10Hz. The input power was fixed at 0.68 J and the output power was measured as 4.4mJ, which was compared to output 8.8 mJ of standard KDP. The diffusion of bright green radiation of wavelength $\lambda=532 \text{ nm}$ ($P_{2\omega}$) by the sample confirms second harmonic generation (SHG). The powder SHG efficiency of BTSCD crystal was about 0.55 times of KDP. The good second harmonic generation efficiency indicates that the BTSCD crystals can be used as a suitable material for non-linear optical devices.

3.7. Vicker's Microhardness test

Mechanical strength of the materials plays a key role in device fabrication. According to Jiang et al. [21], during an indentation process, the external work applied by the indenter is converted to a strain energy component which is proportional to the volume of the resultant impression. The hardness of a material is influenced by various parameters such as the lattice energy, Debye temperature, heat of formation and inter atomic spacing. The Vickers hardness indentations were made on the cut and polished samples of BTSCD of the crystals grown by slow evaporation method.

At room temperature, the load was varied as, 25, 50 and 100 g and the Several indentations were made for each load and the diagonal lengths (d) of the indented impressions were measured using Vickers hardness tester (LEITZ WETZLER) fitted with Vickers diamond indenter and

attached to an incident light.. Vicker's hardness number [22,23] was determined using the formula $H_v = 1.8544 P/d^2$ Kg/mm². The variation of hardness H_v with load P for BTSCD crystal are shown in Figure 9. A plot between $\log p$ vs. $\log d$ for the grown crystal is shown in Figure 10.

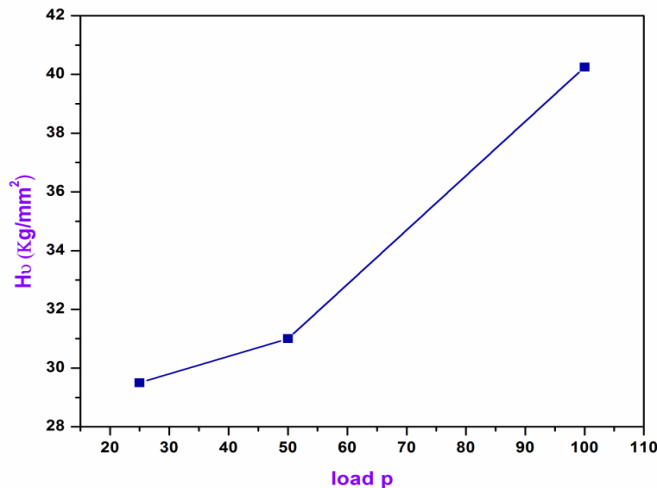


Figure 9. The variation of hardness H_v with load P for BTSCD crystal

The plot between $\log p$ and $\log d$ yields a straight line graph, and its slope gives the work hardening index n , which is found to be $n = 1.7$ for grown BTSCD crystal. According to Onitsch [24], the value of 'n' should lie below 1.6 for comparatively hard materials, whereas it is above 1.6 for softer ones. The microhardness study indicates that the crystal belongs to the class of soft materials.

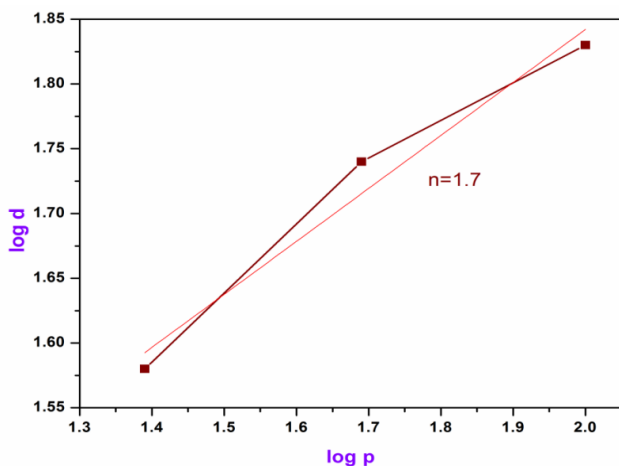


Figure 10. A plot between $\log p$ vs. $\log d$ for BTSCD crystal

3.8. Dielectric Studies

The dielectric constant and the dielectric loss of the BTSCD sample were measured using HIOKI 3532-50 LCR HITESTER. Dielectric constant and dielectric loss of the sample have been measured for different frequencies (100 Hz to 5 MHz) at

different temperatures (308 to 368 K). Figure 11 and Figure 12 show the variations of dielectric constant and dielectric loss respectively as a function of frequency at different temperatures. It is observed from Figure 11 that the dielectric constant (at 308 K) decreases with increase in frequency from 100 Hz to 10 kHz and then attains a constant value of 27.82.

The same trend is observed for other temperatures too. It is also observed that the value of dielectric constant increases with temperature. Such variations at higher temperature may be attributed to the blocking of charge carriers at the electrodes. The decrease of dielectric constant at low frequency region may be due to space charge polarization. Figure 12 indicates that as the frequency increases, the dielectric loss decreases exponentially and then attains a lower value of 0.049 at 308 K. The low value of dielectric loss confirms that the sample possesses lesser defects.

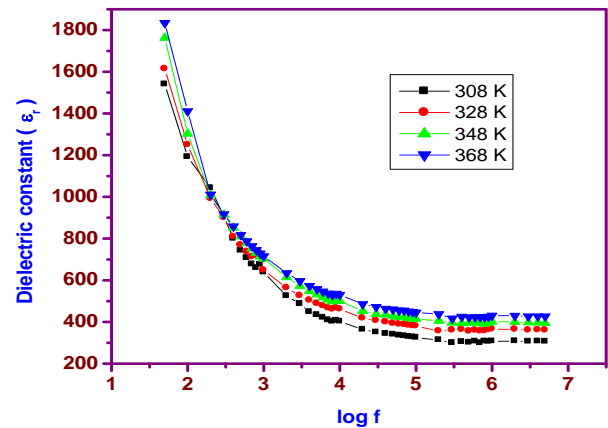


Figure 11. Variation of dielectric constant with log frequency for BTSCD crystal

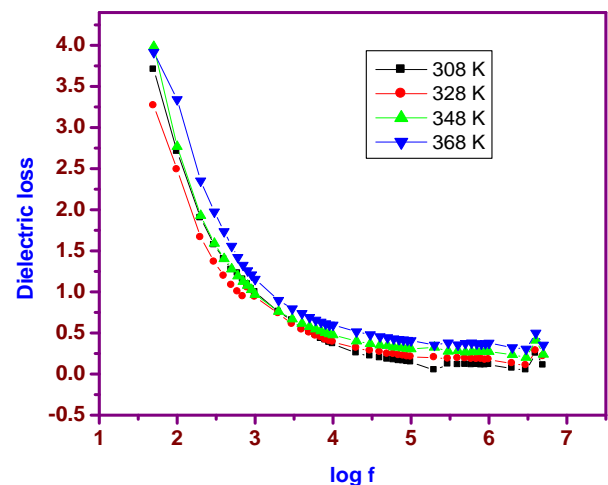


Figure 12. Variation of dielectric loss with log frequency for BTSCD crystal

4. CONCLUSION

A good quality, optically transparent BTSCD crystal has been grown successfully by slow evaporation solution growth technique at room temperature. The unit cell parameters are calculated using Single crystal X-ray diffraction analysis. The grown BTSCD crystal crystallizes in orthorhombic crystal system. Powder XRD shows good crystalline nature of the as grown crystal. The presences of various functional groups in the grown crystal are identified by FT-IR spectrum. . UV-visible analysis was carried out to determine the lower cut off wavelength at 214 nm. Also optical constants like Band gap ($E_g=5.1\text{eV}$), Refractive index ($n=1.6$), Reflectance, Extinction coefficient and Electric susceptibility were determined from UV-VIS-NIR spectrum. The powder SHG efficiency analysis shows that the efficiency of BTSCD crystal is 0.55 times than that of KDP. The mechanical behavior reveals that the BTSCD crystal belongs to soft category. The dielectric studies show that the dielectric constant and dielectric loss of the crystal decreases exponentially with increase in frequency and same trend were observed for different temperatures.

REFERENCES

- I. Ledoux, Synth, Metal, Vol. 54 (1993) pp. 123-137.
1. M. Iwai, T. Kobayashi, H. Furya, Y. Mori, T. Sasaki, Jpn. J. Appl. Phys, Vol. 36 (1997).
2. S. Chenthamarai, D. Jayaraman, P.M. Ushashree, K. Meera, C. Subramanian, P. Ramasamy, Mater. Chem. Phys, Vol. 64 (2000) pp. 179.
3. M. Kitazawa, R. Higuchi, M. Takuhashi, Appl. Phys. Letter, Vol. 64 (1994) pp. 2477.
4. L. Misoguti, A.T. Varela, F.D. Nunes, V.S. Bagnato, F.E.A. Melo, J. Mendes Filho, C. Zilio, Opt. Mater, Vol. 6 (1996) pp. 147.
5. T. Baraniraj, P. Philominathan, Spectrochimica Acta Part A, Vol. 75 (2010) pp. 74-76.
6. N. Zhang, M.H. Jinang, D.R. Yuan, D. Xu, X.T. Tao, Z.S. Shao, J. Cryst. Growth, Vol. 102 (1990) pp. 581.
7. P.R. Newman, L.F. Warren, P. Cunningham, T.Y. Chung, D.E. Copper, G.I. Burdge, P. Polak Dingles, C.K. Lowe Ma, Mater. Res. Soc. Symp.pro, Vol. 173 (1990) pp. 557.
8. M. Ouarsaid, P. Becker, C. Carabatos Nedelec, Phys. Stat. Sol (b), Vol. 207 (1998) pp. 499.
9. S. Selvakumar, J. Packiam Julius, S.A. Rajasekar, A. Ramanand, P. Sagayaraj, Mater. Chem. Phys, Vol. 89 (2005) pp. 244.
10. S.B. Monaco, L.E. Davis, S.P. Velsko, F.T. Wang, D. Eimerl, A. Zalkin, J. Cryst. Growth, Vol. 85 (1987) pp. 252.
11. D. Eimerl, S. Velsko, L. Davis, F. Wang, G. Loiacono, G. Kennedy, IEEEJ. Quantum Electron, Vol. 25 (1989) pp. 179-193.
12. S. Dhanuskodi, J. Ramajothi, Res. Technol, Vol. 39 (2004) pp. 592-597.
13. S. Dhanuskodi, K. Vasantha, P.A. Angelina Mary, Spectrochimica Acta A, Vol. 66 (2007) pp. 637-642.
14. K. Kirubavathi, K. Selvaraju, R. Valluvan, N. Vijayan, S. Kumaraman, Spectrochimica Acta A, Vol. 69 (2008) pp. 1283-1286.
15. J.F. Nicoud, R.J. Twieg, D.S. Chemla, J.E. Zyss (Eds), Academic press, London (1987).
16. R. Christian, solvents and solvent effects in organic chemistry, VCH, New York, 1990.
17. D.D.O Eya, A.J. Ekpunobi, C.E Okeke, Acad. Open Internet. J. 17 (2006).
18. K.Kumar, K.Ramamoorthy, P.M.Koinkar, R.Chandramohan, K.Sankaranarayanan, J.Cryst. Growth 289 (2006)405-407.
19. B.K.Periyasamy, R.S. Jebas, N.Gopalakrishnan, T.Balasubramanian, Mater. Lett. 61 (2007) 4246-4249.
20. Jiang M H., Fang Q., 'Organic and Semiorganic Nonlinear Optical Materials', Adv. Mater, Vol. 11 (1999) pp. 1147-1151.
21. K.G. Subhadra, K. Krishnan Rao, D.B. Sirdeshmukh, Bull. Mater. Sci, Vol. 23 (2000) pp. 147-150.
22. S. Mukerji, T. Kar, Cryst. Res. Technol. Vol. 34 (1999) pp. 1323.
23. Onitseh, E M., 'The present status of testing the hardness of materials', Mikroskopie, Vol. 95 (1956) pp. 12-14.